PROPAGATION OF SHOCK WAVES IN A POLYTROPE WITH A POLOIDAL MAGNETIC FIELD

By Narendra K. Sinha*

[*Manuscript received February* 13, 1968]

Summary

The propagation of a spherically developed shock wave in a polytrope with a poloidal magnetic field has been studied using a generalization of Whitham's method. The effect of the magnetic field on the geometry of the front as well as on the effects brought about by the shock has been discussed.

I. Introduction

The propagation of shock waves in nonuniform compressible media with or without magnetic fields has been considered by a number of authors (Kopal 1954; Rogers 1956; Mackie and Weir 1960; Ôno, Sakashita, and Yamazaki 1960*a*, 1960*b*; and others). In most cases, even though attention has been confined to problems in which physical variables depend upon one spatial coordinate and time, recourse has had to be made to various approximate methods, one of the most useful of which is that first described explicitly by Whitham (1958). Whitham first writes the equation of motion in characteristic form and then applies the differential relation that must be satisfied by flow quantities along a certain characteristic to these flow quantities just behind the shock. When the shock relations are used, a differential equation results for the propagation of the shock. If the appropriate characteristic is chosen, the method gives accurate results for a wide class of problems and shock strengths. Sakashita and Tanaka (1962), Bird (1964), Bhatnagar and Sachdev (1966), and other authors have applied Whitham's method to study the propagation of shock in stellar media with a view to explaining certain astrophysical phenomena.

However, very few investigations have been made on the propagation of a shock in a stellar model with a magnetic field. A magnetic field is known to exist in stellar bodies and a shock wave propagates in a much more complicated way in the presence of a magnetic field. Together with other novel features, there is in general an anisotropy involved in this case. The difficulties inherent in the solution of problems of shock propagation in nonuniform regions are thus sharply accentuated. Even in the simple case when there is only a poloidal magnetic field present the flow quantities are functions of three independent variables.

In the present paper Whitham's rule has been generalized in order to be able to deal with such problems. As in Whitham's method the differential equations are written in characteristic form. However, there is an important difference involved here, in that Whitham's characteristic equations are ordinary differential equations whereas in the present case the equations for the characteristic manifolds are first-order partial differential equations. The approximation used here is to assume that

* Department of Mathematics, Monash University, Clayton, Vic. 3168.

the motion of the shock is identical with the motion of the fast outward magneto-acoustic wave. The partial differential equations involved are solved by using the method of bicharacteristics. A detailed discussion of this method can be found in Jeffrey and Taniuti (1964).

The problem of finding suitable stellar models with magnetic fields is still under investigation and detailed results are not available. Studies on the structure of magnetic fields in a polytrope have been made, however, as a first step towards the solution of the problem of magnetic fields in real stars. In the absence of such a solution, we use the polytropic solutions to illustrate a method of dealing with shock waves in magnetic stars. Roxburgh (1966) has discussed the poloidal magnetic field structure in polytropes without any internal motion. We take his solution (Section III) as our equilibrium solution of the polytropic star and illustrate the propagation of shock waves in this medium.

We have not discussed the mechanism of the generation of shock waves in the stellar interiors, but its possibility cannot be ruled out. For example, any rapid expansion of the core brought about by nuclear reactions may induce a shock wave. In fact, shock waves are at present associated with some interesting astrophysical phenomena like novae and supernovae explosions, gas motions in the chromosphere, etc. Ôno and Sakashita (1961) have quantitatively used shock waves to explain the mechanism of supernovae explosions.

II. Basic Equations

Since we are only considering poloidal magnetic fields here, the magnetic induction $\boldsymbol{B}$ and the fluid velocity $\boldsymbol{v}$ may be written as

$$\boldsymbol{B} = \boldsymbol{e}_r B_r + \boldsymbol{e}_z B_z\,, \qquad \text{and} \qquad \boldsymbol{v} = \boldsymbol{e}_r u_r + \boldsymbol{e}_z u_z\,,$$

where r, ϕ, z are cylindrical coordinates and $\boldsymbol{e}_r, \boldsymbol{e}_\phi, \boldsymbol{e}_z$ the corresponding unit vectors. The origin of the coordinates has been supposed to be at the centre of the polytrope and the z axis along the axis of symmetry. Furthermore, it is clear that, with poloidal fields, $\boldsymbol{v}$ and $\boldsymbol{B}$ as well as the density ρ and the pressure p will depend only upon r, z, and t. Then assuming that the viscosity is negligible, the conductivity infinite, and the medium a perfect fluid, the Lundquist equations (Jeffrey and Taniuti 1964) reduce to the following system of quasi-linear hyperbolic partial differential equations:

$$\frac{\partial\rho}{\partial t} + u_r\frac{\partial\rho}{\partial r} + u_z\frac{\partial\rho}{\partial z} + \rho\frac{\partial u_r}{\partial r} + \rho\frac{\partial u_z}{\partial z} + \rho\frac{u_r}{r} = 0\,, \tag{1}$$

$$\rho\frac{\partial u_r}{\partial t} + \rho u_r\frac{\partial u_r}{\partial r} + \rho u_z\frac{\partial u_r}{\partial z} + \frac{\partial p}{\partial r} + \frac{B_z}{\mu}\frac{\partial B_z}{\partial r} - \frac{B_z}{\mu}\frac{\partial B_r}{\partial z} = -\rho\frac{\partial\Psi}{\partial r}\,, \tag{2}$$

$$\rho\frac{\partial u_z}{\partial t} + \rho u_r\frac{\partial u_z}{\partial r} + \rho u_z\frac{\partial u_z}{\partial z} + \frac{\partial p}{\partial z} + \frac{B_r}{\mu}\frac{\partial B_r}{\partial z} - \frac{B_r}{\mu}\frac{\partial B_z}{\partial r} = -\rho\frac{\partial\Psi}{\partial z}\,, \tag{3}$$

$$\frac{\partial B_r}{\partial t} + u_r\frac{\partial B_r}{\partial r} + u_z\frac{\partial B_r}{\partial z} - B_z\frac{\partial u_r}{\partial z} + B_r\frac{\partial u_z}{\partial z} + \frac{B_r u_r}{r} = 0\,, \tag{4}$$

$$\frac{\partial B_z}{\partial t} + u_r\frac{\partial B_z}{\partial r} + u_z\frac{\partial B_z}{\partial z} - B_r\frac{\partial u_z}{\partial r} + B_z\frac{\partial u_r}{\partial r} + \frac{B_z u_r}{r} = 0\,, \tag{5}$$

$$\rho\frac{\partial p}{\partial t}+\rho u_r\frac{\partial p}{\partial r}+\rho u_z\frac{\partial p}{\partial z}-\gamma p\frac{\partial \rho}{\partial t}-\gamma p u_r\frac{\partial \rho}{\partial r}-\gamma p u_z\frac{\partial \rho}{\partial z}=0\,, \tag{6}$$

where Ψ is the gravitational potential. The entropy relation $S = S_0 + C_v \ln(p\rho^{-\gamma})$ has been assumed. Further Ψ satisfies Poisson's equation

$$\frac{\partial^2\Psi}{\partial r^2}+\frac{1}{r}\frac{\partial\Psi}{\partial r}+\frac{\partial^2\Psi}{\partial z^2}=4\pi G\rho\,. \tag{7}$$

Since the motion is axisymmetrical, we discuss the motion in an azimuthal plane only.

III. Equilibrium Solution

Roxburgh (1966) has considered dipole solutions $\bar{S}(R,\theta) = A(R)\sin^2\theta$, expressing the field as

$$\boldsymbol{B} \equiv \left(\frac{2A\cos\theta}{R^2}, -\frac{\mathrm{d}A}{\mathrm{d}R}\frac{\sin\theta}{R}, 0\right), \tag{8}$$

in the spherical coordinates (R,θ,ϕ), θ being the angle made with the z axis. $\bar{S}$ = constant are the field lines of $\boldsymbol{B}$. The equation determining A comes out to be

$$\frac{\mathrm{d}^2A}{\mathrm{d}R^2}-\frac{2A}{R^2}+D\rho R^2=0\,, \tag{9}$$

where D is a constant. Using the transformations

$$\left.\begin{aligned} R &= a\xi\,, & A &= D\rho_{\mathrm{c}}a^4\bar{\gamma}\,,\\ \rho_0 &= \rho_{\mathrm{c}}\theta_0^n\,, & a &= \{K(n+1)\rho_{\mathrm{c}}^{n^{-1}-1}/4\pi G\}^{\frac{1}{2}}\,, \end{aligned}\right\} \tag{10}$$

where the symbols have their usual meanings, equation (9) reduces to

$$\frac{\mathrm{d}^2\bar{\gamma}}{\mathrm{d}\xi^2}-\frac{2\bar{\gamma}}{\xi^2}=-\theta_0^n\,\xi^2\,. \tag{11}$$

For the polytrope $n = 1$, $\theta_0 = (\sin\xi)/\xi$ and therefore $\xi = \pi$ defines the surface of the polytrope. With the boundary conditions

$$\bar{\gamma}=\mathrm{d}\bar{\gamma}/\mathrm{d}\xi=0 \qquad \text{at} \qquad \xi=0$$

and

$$\xi\,\mathrm{d}\bar{\gamma}/\mathrm{d}\xi+\bar{\gamma}=0 \qquad \text{at} \qquad \xi=\pi\,,$$

equation (11) is found to have the solution

$$\bar{\gamma}=\tfrac{1}{3}\xi^2+\xi\sin\xi+2\cos\xi-(2\sin\xi)/\xi\,,$$

which is not in agreement with the solution given by Roxburgh (equation (29) in his paper; the variable $\bar{\gamma}$ here is the same as γ of Roxburgh).

The structure of the magnetic field in the polytrope is now known. The resolutes of $\boldsymbol{B}$ corresponding to the field (8) are

$$B_r=\frac{Jrz(3Q-1-\cos\xi)}{r^2+z^2}\,, \qquad B_z=\frac{J\{(2z^2-r^2)Q+(1+\cos\xi)r^2\}}{r^2+z^2}\,, \tag{12}$$

where

$$Q = \frac{1}{3} + \frac{\sin\xi}{\xi} + \frac{2\cos\xi}{\xi^2} - \frac{2\sin\xi}{\xi^3},$$

and

$$J = \rho_c a^2 D$$

is a constant that is proportional to the strength of the magnetic field. The null point of the field is located at $\xi = 2\cdot4035$ approximately on the r axis. The field lines form closed loops about the null point, in the clockwise sense, in an azimuthal plane. On $\xi =$ constant the magnitude of the field (Fig. 1), as well as its inclination with the r axis, decreases as θ increases. Moreover, $B_r = 0$ when either $r = 0$ or $z = 0$, so that at points on the axes the field is parallel to the z axis.

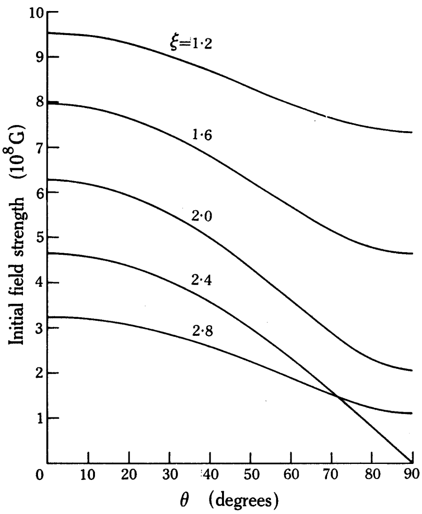

Fig. 1.—Initial distribution of field strength on curves $\xi =$ constant in the upper half of the azimuthal plane; $\mathscr{S}_0 = 0\cdot707$ (Section VI).

Furthermore, p and ρ, which are spherically symmetric to the first approximation, are given by

$$p = k\rho^2, \qquad \rho = \rho_c(\sin\xi)/\xi,$$

where ξ is expressed as

$$\xi = (r^2+z^2)^{\frac{1}{2}}/a.$$

IV. Shock Relations

Equations (1)–(6), being a system of quasi-linear hyperbolic partial differential equations, admit of weak solutions in which the values of the physical quantities p, ρ, $\boldsymbol{v}$, and $\boldsymbol{B}$ may be discontinuous across certain surfaces called shock fronts. (Since the gravitational potential Ψ satisfies the elliptic equation (7), it will be analytic throughout the whole region.) The equations connecting the values of the physical quantities on each side of the shock front are obtained by writing the equations (1)–(6) in conservation form (Jeffrey and Taniuti 1964), and in the present case they are

$$U(\rho-\rho_0) = \rho u_n, \tag{13a}$$

$$U(B_e-B_{e0}) = B_e u_n - B_n u_e, \tag{13b}$$

$$B_n = B_{n0}, \tag{13c}$$

$$U\rho u_n = \rho u_n^2+(p-p_0)+(1/2\mu)(B^2-B_0^2), \tag{13d}$$

$$U\rho u_e = \rho u_e u_n - (1/\mu)(B_e-B_{e0})B_n, \tag{13e}$$

$$U\left(\tfrac{1}{2}\rho u^2+\frac{p-p_0}{\gamma-1}+\frac{1}{2\mu}(B^2-B_0^2)\right) = u_n\left(\tfrac{1}{2}\rho u^2+\frac{\gamma p}{\gamma-1}+\frac{B^2}{\mu}\right)-\frac{B_n}{\mu}\left(B_n u_n+B_e u_e\right), \tag{13f}$$

where U is the absolute normal velocity of the shock front. The subscript 0 refers to the region at rest ahead of the shock and variables without it refer to the shocked region. Further, the subscripts n and e give the components normal and tangential to the shock front respectively in the azimuthal plane. The values of the physical quantities behind the shock may now be expressed in terms of those ahead of the shock and the shock strength λ as

$$\rho = \lambda\rho_0, \tag{14a}$$

$$u_n = (1-1/\lambda)U, \tag{14b}$$

$$u_e = (1-\lambda)B_n B_{e0}\, U/(U^2\mu\rho_0-\lambda B_n^2), \tag{14c}$$

$$B_n = B_{n0}, \tag{14d}$$

$$B_e = (U^2\mu\rho_0-B_n^2)\lambda B_{e0}/(U^2\mu\rho_0-\lambda B_n^2), \tag{14e}$$

$$p = p_0+\left(1-\frac{1}{\lambda}\right)U^2\rho_0-\left(U^2\mu\rho_0-\lambda B_n^2+\lambda(U^2\mu\rho_0-B_n^2)\right)\frac{(\lambda-1)U^2B_{e0}^2\rho_0}{2(U^2\mu\rho_0-\lambda B_n^2)^2}, \tag{14f}$$

where U itself is given by the equations

$$U = 0, \qquad \text{or} \qquad U^6-E_1U^4+E_2U^2-E_3 = 0, \tag{15}$$

E_1, E_2, and E_3 being known functions of the physical quantities ahead of the shock. The r and z components of the physical quantities behind the shock are easily obtained from equations (14) by the transformations

$$F_r = \frac{h_r F_n - h_z F_e}{(h_r^2+h_z^2)^{\frac{1}{2}}} \qquad \text{and} \qquad F_z = \frac{h_z F_n + h_r F_e}{(h_r^2+h_z^2)^{\frac{1}{2}}}.$$

The speeds U of propagation given by (15) correspond to the various discontinuities that exist in a magnetohydrodynamic medium. The case $U = 0$ corresponds to a contact discontinuity and is immediately ruled out. The second equation in (15) is a cubic in U^2 and gives the speeds of the fast, slow, and intermediate shocks. This equation may be rewritten as

$$E^{\mathrm{I}}\lambda^3-E^{\mathrm{II}}\lambda^2+E^{\mathrm{III}}\lambda-E^{\mathrm{IV}} = 0, \tag{16}$$

where

$$E^{\mathrm{I}} = \{(\gamma-1)\mu U^2 B_0^2 \rho_0 + 2\gamma\mu B_{\mathrm{n}}^2 p_0\} B_{\mathrm{n}}^2 ,$$

$$E^{\mathrm{II}} = \{(\gamma+1)B_0^2 + 4\gamma\mu p_0\}\mu U^2 B_{\mathrm{n}}^2 \rho_0 - \{(2-\gamma)B_0^2 - \gamma B_{\mathrm{n}}^2\}\mu^2 U^4 \rho_0^2 ,$$

$$E^{\mathrm{III}} = \{(\gamma-1)\mu U^2 \rho_0 + 2\gamma\mu p_0 + (\gamma+2)B_{\mathrm{n}}^2 + \gamma B_0^2\} U^4 \mu^2 \rho_0^2 ,$$

$$E^{\mathrm{IV}} = (\gamma+1)\mu^3 U^6 \rho_0^3 .$$

The equation (16) is a cubic in λ and gives the strength of the fast, slow, and intermediate shocks that correspond to a given speed U of propagation. To find the root λ_{f}, corresponding to the fast shock, the evolutionary conditions for a physically relevant shock are invoked. The intermediate shock is noncompressive and therefore the corresponding λ is less than or equal to unity. Such a root is discarded. Furthermore, we note that a fast shock brings about an increase in the magnitude of the tangential component of the magnetic field, whereas the latter is decreased on the passage of a slow shock. We use this property to isolate λ_{f}. However, when $B_{\mathrm{n}} = 0$, perpendicular shock locally, equation (16) reduces to the quadratic equation in λ

$$(2-\gamma)b_0^2\lambda^2 + \{(\gamma-1)U^2 + 2c_0^2 + \gamma b_0^2\}\lambda - (\gamma+1)U^2 = 0 , \tag{17}$$

where $c^2 = \gamma p/\rho$ is the square of the sound speed and $\boldsymbol{b} = (\mu\rho)^{-\frac{1}{2}}\boldsymbol{B}$ is the Alfven velocity vector. One of the roots of equation (17) is positive and the other is negative. Since U^2 is greater than $c_0^2 + b_0^2$, the positive root is greater than unity and gives λ_{f} in this case. Similarly, when $\gamma = 2$ the only remaining root is greater than unity and corresponds to λ_{f}.

Thus U and the state ahead of the shock being known, the value of λ_{f} can be obtained and then the values of the physical quantities behind the shock can be determined with the help of equations (14).

V. Generalized Whitham's Method using Characteristic Manifolds

If $h(r,z,t) = 0$ is the equation of a characteristic manifold, across which there may be discontinuities in the derivatives of p, ρ, $\boldsymbol{v}$, and $\boldsymbol{B}$, then we get the equation (Courant and Friedrichs 1948)

$$\left(\frac{\mathrm{d}h}{\mathrm{d}t}\right)^2\left\{\left(\frac{\mathrm{d}h}{\mathrm{d}t}\right)^4 - (c^2+b^2)(h_r^2+h_z^2)\left(\frac{\mathrm{d}h}{\mathrm{d}t}\right)^2 + c^2(h_r^2+h_z^2)\frac{(B_r h_r + B_z h_z)^2}{\mu\rho}\right\} = 0 \tag{18}$$

for the characteristic manifolds, where

$$\frac{\mathrm{d}}{\mathrm{d}t} \equiv \frac{\partial}{\partial t} + u_r\frac{\partial}{\partial r} + u_z\frac{\partial}{\partial z} ,$$

and the subscripts on h indicate partial derivatives. The equation (18) shows the existence of the following three real characteristic manifolds.

$$\mathrm{d}h/\mathrm{d}t = 0 , \tag{19}$$

$$(\mathrm{d}h/\mathrm{d}t)^2 - \tfrac{1}{2}(h_r^2+h_z^2)(c^2+b^2+\eta) = 0 , \tag{20}$$

$$(\mathrm{d}h/\mathrm{d}t)^2 - \tfrac{1}{2}(h_r^2+h_z^2)(c^2+b^2-\eta) = 0 , \tag{21}$$

where

$$\eta = +\{(c^2+b^2)^2-\nu\}^{\frac{1}{2}}, \qquad \text{with} \qquad \nu = \frac{4c^2}{\mu\rho}\frac{(B_r h_r + B_z h_z)^2}{(h_r^2+h_z^2)}.$$

Equation (19) simply means that the particle paths are bicharacteristics, i.e. they generate a characteristic manifold. The characteristic manifolds given by equations (20) and (21) are the fast and slow magnetoacoustic wave fronts respectively.

The equation for the outward moving fast magnetoacoustic wave $h(r,z,t) = 0$ is obtained as

$$h_t + u_r h_r + u_z h_z + \{\tfrac{1}{2}(h_r^2+h_z^2)(c^2+b^2+\eta)\}^{\frac{1}{2}} = 0. \tag{22}$$

The characteristic rays in this case are given by the following system of differential equations.

$$\frac{dr}{dt} = u_r + \frac{1}{\eta_3}\left(\eta_2 h_r - \frac{2\eta_1 c^2 h_z}{\eta}\right), \tag{23}$$

$$\frac{dz}{dt} = u_z + \frac{1}{\eta_3}\left(\eta_2 h_z + \frac{2\eta_1 c^2 h_r}{\eta}\right), \tag{24}$$

$$\frac{dh_r}{dt} = -h_r\frac{\partial u_r}{\partial r} - h_z\frac{\partial u_z}{\partial r} + \eta_4\frac{\partial p}{\partial r} + \eta_5\frac{\partial \rho}{\partial r} + \eta_6\frac{\partial B_r}{\partial r} + \eta_7\frac{\partial B_z}{\partial r}, \tag{25}$$

$$\frac{dh_z}{dt} = -h_r\frac{\partial u_r}{\partial z} - h_z\frac{\partial u_z}{\partial z} + \eta_4\frac{\partial p}{\partial z} + \eta_5\frac{\partial \rho}{\partial z} + \eta_6\frac{\partial B_r}{\partial z} + \eta_7\frac{\partial B_z}{\partial z}, \tag{26}$$

$$\frac{dh_t}{dt} = -h_r\frac{\partial u_r}{\partial t} - h_z\frac{\partial u_z}{\partial t} + \eta_4\frac{\partial p}{\partial t} + \eta_5\frac{\partial \rho}{\partial t} + \eta_6\frac{\partial B_r}{\partial t} + \eta_7\frac{\partial B_z}{\partial t}, \tag{27}$$

where

$$\eta_1 = (B_r h_r + B_z h_z)(B_r h_z - B_z h_r)/(h_r^2+h_z^2)\mu\rho,$$

$$\eta_2 = c^2+b^2+\eta,$$

$$\eta_3 = +2\{\tfrac{1}{2}(h_r^2+h_z^2)\eta_2\}^{\frac{1}{2}},$$

$$\eta_4 = (h_r^2+h_z^2)(\nu-2c^2\eta_2)/4p\eta\eta_3,$$

$$\eta_5 = (h_r^2+h_z^2)(c^2\eta_2+b^2\eta_2-\nu)/2\rho\eta\eta_3,$$

$$\eta_6 = \left(h_r^2+h_z^2\right)\left(\frac{\nu h_r}{2(B_r h_r + B_z h_z)\eta\eta_3} - \frac{\eta_2 B_r}{\mu\rho\eta\eta_3}\right),$$

$$\eta_7 = \left(h_r^2+h_z^2\right)\left(\frac{\nu h_z}{2(B_r h_r + B_z h_z)\eta\eta_3} - \frac{\eta_2 B_z}{\mu\rho\eta\eta_3}\right).$$

The position and orientation of the wave front are thus known if the system of equations (23)–(26) can be solved. An exact solution is not possible and, in general, numerical integration has to be employed. The method to determine the motion of the shock wave is to assume that the motion of the shock wave is identical with the motion of the outward moving fast magnetoacoustic wave with which the shock originally coincided. In this case the various physical quantities occurring in the second members of the equations (23)–(26) are related to the physical quantities ahead of the shock by the shock relations (13). Since the medium ahead of the shock is independent of time, it follows from equation (27) that h_t is constant.

The speed U of the wave front is given by

$$U = -h_t/(h_r^2+h_z^2)^{\frac{1}{2}},$$

where h_t is now constant. If the initial values of h_r and h_z are chosen so that $h_r^2+h_z^2 = 1$, then $-h_t = U_0$, the initial value of U, and we get

$$U = U_0/(h_r^2+h_z^2)^{\frac{1}{2}}. \tag{28}$$

The shock is moving in an inhomogeneous medium and in a nonuniform magnetic field. Consequently, the orientation of the shock front as well as its velocity will be changing as it moves onwards. Equation (28) serves to give the value of the normal velocity of the wave front at any time at any point.

VI. Numerical Integration

The central density and the radius of the polytrope under consideration ($n = 1$), which are independent of each other in this case, have been assumed to be identical with the solar values, so that

$$\rho_c = 75\cdot 858 \qquad \text{and} \qquad \bar{R} = 6\cdot 951\times 10^{10},$$

(in CGS units) where $\bar{R}$ is the radius. (We use CGS units throughout the calculation.) From equations (10) it is then found that

$$a = 2\cdot 212\times 10^{10} \qquad \text{and} \qquad K = 2\cdot 052\times 10^{14}.$$

The shock is assumed to develop and start spherically outwards at the surface $\xi = 1$. On this surface it is found that $J \simeq 1\cdot 26\times 10^9\, \mathscr{S}_0$, where $\mathscr{S} = b/c$ is a non-dimensional parameter. Shocks of different initial intensity, corresponding to Mach number $M_{s,i}$ ($\equiv U_0/C_0$) $= 1\cdot 25$, 2, 3, and 5 have been considered and the propagation of each of them studied for different strengths of the field (12). The magnetic field encountered in astrophysical problems is generally weak and hence it has been chosen to correspond to the values $0\cdot 3$, $0\cdot 5$, and $0\cdot 707$ of $\mathscr{S}_0$ at $\xi = 1$. For these characteristic values the field is about 10^8 G, which agrees well with its estimated value in the stellar interiors. $M_{s,i}$ is limited to 5 because we have confined studies here to nonrelativistic and physically realistic phenomena. Knowledge of $M_{s,i}$ helps to obtain the value of U_0, and that of $\mathscr{S}_0$ at $\xi = 1$ helps to determine J. When J is known the poloidal field (12) is specified completely.

With these initial and other relevant data equations (23)–(26) have been integrated in conjunction with equation (28) using the Runge–Kutta method on a CDC 3200 computer, with time steps $\Delta t = 0\cdot 1$. After every 100 steps of integration the values of the physical quantities just behind the shock were computed with the help of equations (14). Since the magnetic field is dipole in nature, the values of the physical quantities must be symmetrical about the r axis. This follows also from the fact that the set of equations (1)–(6) is invariant under the transformation ($z \to -z, u_z \to -u_z, B_r \to -B_r$). Therefore the computation has been carried out only in the upper half of the azimuthal plane (r–z quadrant), carrying it nearly as far out as the surface. Furthermore, the initial shock position now becomes a quadrant of the circle $\xi = 1$.

The results of the foregoing integration give the characteristic rays through any prescribed values of r, z, h_r, and h_z, considering this set as the initial values. The integration has been done for 19 different points on the initial shock position at 5° intervals of θ, unfolding the characteristic ray in each case. The position of the front, at any subsequent time t, in the quadrant is obtained as the locus of the positions at time t on the different rays. The front is, in general, not circular and we have expressed the different radial distances obtained for the front at any particular time t as the series

$$R_0(t) + R_2(t)\,\mathrm{T}_2(\cos\theta) + R_4(t)\,\mathrm{T}_4(\cos\theta) + \ldots,$$

where $\mathrm{T}_n(\omega) = \cos(n\cos^{-1}\omega)$ are the Chebyshev polynomials. Owing to the symmetry of the problem about the r axis and the parity property of these polynomials, only even terms appear in the expansion. The first term $R_0(t)$ gives the mean radius of the front at time t, whereas each of the remaining terms introduces a nonspherical distortion. Similarly, the density ratio λ, pressure ratio Π, and ratio β of the magnetic field across the front, as well as the shock Mach number M_s at different times t have also been expressed as the respective series

$$\lambda_0(t) + \lambda_2(t)\,\mathrm{T}_2(\cos\theta) + \lambda_4(t)\,\mathrm{T}_4(\cos\theta) + \ldots,$$

$$\Pi_0(t) + \Pi_2(t)\,\mathrm{T}_2(\cos\theta) + \Pi_4(t)\,\mathrm{T}_4(\cos\theta) + \ldots,$$

$$\beta_0(t) + \beta_2(t)\,\mathrm{T}_2(\cos\theta) + \beta_4(t)\,\mathrm{T}_4(\cos\theta) + \ldots,$$

and

$$M_0(t) + M_2(t)\,\mathrm{T}_2(\cos\theta) + M_4(t)\,\mathrm{T}_4(\cos\theta) + \ldots.$$

As above, the first term in each case gives the mean value of the function over the front at time t whereas the remaining terms introduce the nonspherically symmetric variations in these quantities.

VII. Results and Discussion

As indicated in Section VI, shock waves with different initial parameters have been studied. The physical values recorded in some of the cases are depicted in the figures. The different curves, as also the corresponding cases, are referred according to the following scheme of initial parameters:

Curve/Case	1	2	3	4	5	6
$M_{s,i}$	1·25	1·25	1·25	2·0	3·0	5·0
$\mathscr{S}_0$	0·3	0·5	0·707	0·707	0·707	0·707

The following results about the shock front and the changes in physical variables brought about by the passage of the shock front as it propagates outwards in the polytrope follow from the investigations.

(i) *Behaviour of* Π

The variations of Π_0 and Π_2 with $\bar{R}_0$, where $\bar{R}_0 = R_0/\bar{R}$, are shown in Figures 2(*a*) and 2(*b*) respectively. Π_2 is small and brings only a small change in Π_0 at different points on the front. This change decreases with decreasing $\mathscr{S}_0$. This is the pure gas-dynamical limit. In the pure gas-dynamical limit ($\mathscr{S}_0 \to 0$) the ratio of the values of any physical variable across the front is uniform over the front. Π_0, and hence Π, continuously amplifies, the amplification being more pronounced with increasing $M_{s,i}$ and less sensitive to small changes in field strength (FS). However,

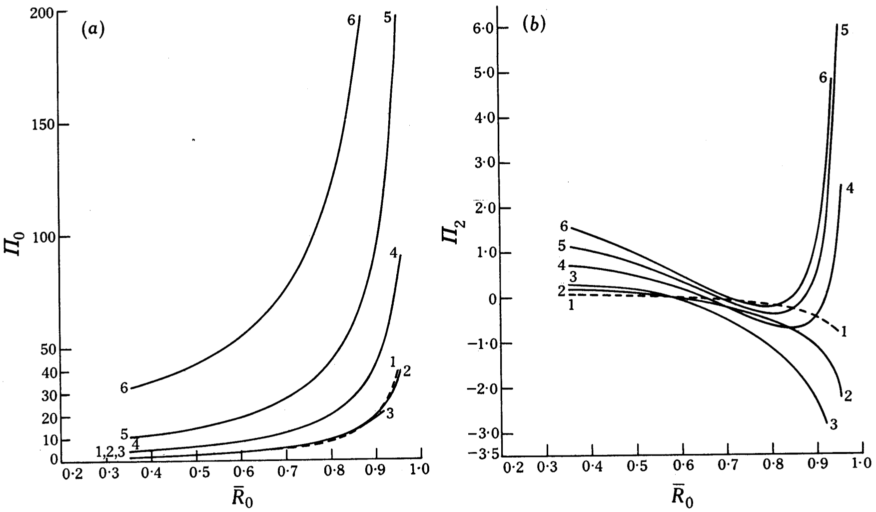

Fig. 2.—Variation of (*a*) Π_0 and (*b*) Π_2 as functions of $\bar{R}_0$ for different initial characteristics.

it does not increase without limit and even for the case (6), Π_0 and Π_2 are only $430 \cdot 9$ and $4 \cdot 8$ at $0 \cdot 94\,\bar{R}_0$. These values are small compared with those obtained by earlier workers in the absence of a magnetic field, for example, Π_0 and Π_2 are only 54 and $-0 \cdot 35$ at $\bar{R}_0 = 0 \cdot 835$ for the case (5) compared with the Π values of 102 and 281 obtained by Bhatnagar and Sachdev (1966) for different models, taking the impoverishment of Π due to radiation into account but excluding any magnetic field. The relatively small growth of Π in the present case is due to the presence of a magnetic field which always inhibits the growth of Π, as can be seen from equations (14).

(ii) *Behaviour of* λ

λ also increases continuously (Fig. 3), but as expected (as $1 < \lambda < (\gamma+1)/(\gamma-1)$) is always less than 3. λ_2 is small compared with λ_0 and becomes vanishingly small as $\mathscr{S}_0$ becomes small, which is the gas-dynamical limit. The results near the surface of the polytrope may be illusory because radiation effects, which are always significant there, have not been included in this paper. The effect of $M_{s,i}$ on λ is more pronounced than that of $\mathscr{S}_0$. Increasing $M_{s,i}$ leads to increasing compression of the matter in the medium, but the gradient is sharper for lower $M_{s,i}$. The change in

FS does not alter λ appreciably. In the early stages, λ is greater for weaker FS but in this case there exist two critical $\bar{R}_0$ values, one at $0 \cdot 575\, \bar{R}_0$ and the other at $0 \cdot 835\, \bar{R}_0$ for $M_{s,i} = 1 \cdot 25$, and λ changes its behaviour after each of these values.

(iii) *Behaviour of* β

The effect of the second term, β_2, is more significant (Fig. 4) in the case of the ratio of the magnetic field. This is due to the nonuniform and anisotropic nature of the poloidal magnetic field. FS, as expected, always increases after the passage of the shock. Taking the contribution of β_2 into account, it is found that β is not very sensitive to the weak changes in $\mathscr{S}_0$. However, β does increase, though not appreciably,

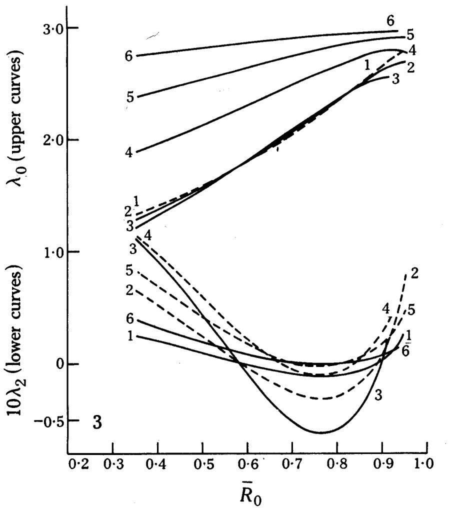

Fig. 3.—Profiles illustrating the density ratio as a function of $\bar{R}_0$ for different initial characteristics.

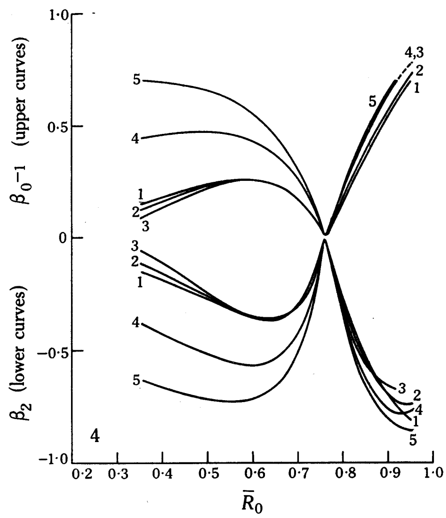

Fig. 4.—Profiles illustrating the field strength ratio as a function of $\bar{R}_0$ for different initial characteristics.

with increasing $M_{s,i}$. The compression of the matter in the medium is basically responsible for the increase in the magnetic field and this explains the above behaviour of β. The null point exists at $0 \cdot 765\, \bar{R}_0$ on the equatorial plane, which explains why all the curves behave critically near this point.

(iv) *Behaviour of* M_s

The shock Mach number M_s also continuously increases (Fig. 5) and does so more and more rapidly as $M_{s,i}$ increases. This agrees with the results of Masani (1963) and Bhatnagar and Sachdev (1966). However, M_s is also not very sensitive to small changes in $\mathscr{S}_0$, but this picture of the shock may be illusory, because the shock moves out in a medium in which the material density is continuously decreasing. In fact, the shock velocity, though always increasing, does so only slightly; for example, the shock velocity changes from $2 \cdot 024$ at $\xi = 1$ to a maximum of only $2 \cdot 29$ in case (1), $2 \cdot 33$ in case (2), and $2 \cdot 4$ in case (4) (in 10^8 units) near the surface. Even in case (6) the shock velocity changes from $8 \cdot 09$ at $\xi = 1$ to only $8 \cdot 13$ near the surface. In fact, it appears that the greater the initial shock velocity (ISV) the less the shock velocity increases towards the surface. This behaviour is in marked contrast to the changes in the shock velocity obtained in the absence of a magnetic field. For example, Ôno, Sakashita, and Yamazaki (1960*a*) have found that in the Eddington model ($M = 1\,M_{\odot}$, $\bar{R} = 0\cdot 1\,R_{\odot}$) the shock velocity increases from an initial value of $2\cdot 1\times 10^8$ at $0\cdot 125\,x$ to $5\cdot 1\times 10^9$ near the surface ($x = 0\cdot 87$). Thus the magnetic field restrains the growth of the shock velocity.

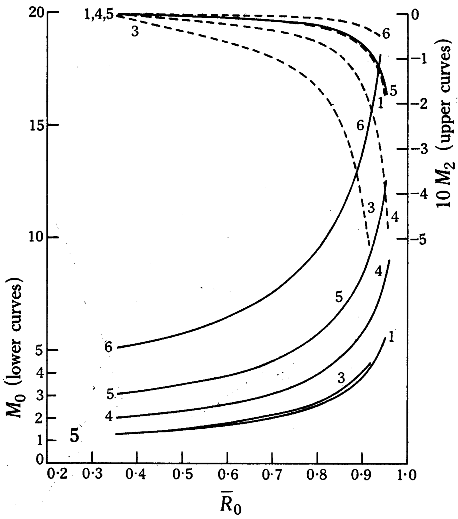

Fig. 5.—Variation of shock Mach numbers as a function of $\bar{R}_0$ for different initial characteristics.

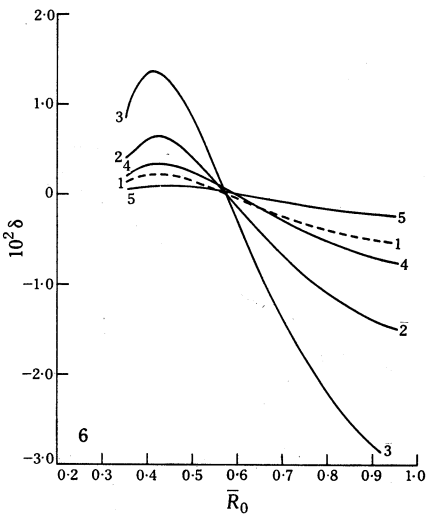

Fig. 6.—Variation of the oblateness of the shock front as a function of $\bar{R}_0$ for different initial characteristics.

(v) *Geometry of the Front*

The coefficients R_{2j} ($j = 1, 2, 3, \ldots$) decrease rapidly so that to a first approximation

$$R = R_0 + R_2\,\mathrm{T}_2(\cos\theta)\,,$$

showing that the front is elliptical. Since the value of $\mathrm{T}_2(\cos\theta)$ is $+1$ along the axis and -1 at the equator, the oblateness δ of the front is given by

$$\delta = 2R_2/R_0\,.$$

The variation of δ with $\bar{R}_0$ has been shown in Figure 6. Both the FS and ISV strongly influence the behaviour of δ. In the early stage of propagation δ increases but soon after it starts to decrease steadily and becomes negative in the outer layers of the polytrope. This behaviour may be attributed to the structure of the magnetic field. The change from positive to negative takes place at the same R_0 for different FS but the same ISV. This critical R_0 differs, though only slightly, for different ISV. Decreasing FS decreases δ, which would vanish in the pure gas-dynamical limit when FS $\to 0$. For a given FS, however, δ decreases with increasing $M_{s,t}$, showing that fronts moving in a given magnetic field are less distorted for more intense shocks.

In other words, the less intense the shock the greater is the time lag of the front in reaching the equator and in reaching successively the points on the surface of the polytrope with increasing latitudes up to the poles. For example, in case (1) it takes $165 \cdot 9$ sec to move to $0 \cdot 97\,\bar{R}_0$ along the axis whereas $158 \cdot 7$ sec only to traverse the same distance in the equatorial plane.

As a result of increasing shock velocity the particle velocity behind the shock also increases as the front propagates outwards. The escape velocity at the surface is given by

$$u_{\mathrm{esc}} = (2GM/R)^{\frac{1}{2}} = 6 \cdot 2 \times 10^{7}\ \mathrm{cm\,sec^{-1}}.$$

This velocity is always attained, in the present case, even for $M_{\mathrm{s},i} = 1 \cdot 25$, so that in general the shock will cause an ejection of mass from the polytrope. The presence of the magnetic field increases the particle velocity, as can be seen from equations (14), and hence the magnetic field increases the possibility of ejection of mass from a stellar body in the event of the generation of a shock wave in it. This may be of importance in novae explosions. For large $M_{\mathrm{s},i}$, u_{esc} is attained well within the star and, in fact, with increasing $M_{\mathrm{s},i}$ the escape velocity is attained nearer and nearer to the centre.

The rise in temperature brought about by the shock may be obtained from the relation

$$T/T_0 = \Pi/\lambda,$$

where T is temperature, and it follows that a poloidal magnetic field inhibits the rise in temperature, i.e. the intense heating of the medium that occurs during the passage of a shock wave. The growth of higher nuclear reactions in the stellar body due to a shock is thus slowed and supernovae explosions are inhibited by the presence of the magnetic field.

VIII. Acknowledgment

The author wishes to thank Dr. E. D. Fackerell for suggesting the problem and for valuable discussions during the progress of this work.

IX. References

Bhatnagar, P. L., and Sachdev, P. L. (1966).—*Nuovo Cim.* **44**, 15.

Bird, G. A. (1964).—*Astrophys. J.* **139**, 675.

Courant, R., and Friedrichs, K. O. (1948).—"Supersonic Flow and Shock Waves." (Interscience: New York.)

Jeffrey, A., and Taniuti, T. (1964).—"Non-linear Wave Propagation." (Academic Press: New York.)

Kopal, Z. (1954).—*Astrophys. J.* **120**, 159.

Mackie, A. G., and Weir, D. G. (1960).—*Proc. Camb. phil. Soc.* **56**, 64.

Masani, A. (1963).—*Nuovo Cim.* **29**, 224.

Ôno, Y., and Sakashita, S. (1961).—*Publs astr. Soc. Japan* **13**, 146.

Ôno, Y., Sakashita, S., and Yamazaki, H. (1960*a*).—*Prog. theor. Phys., Kyoto* **23**, 294.

Ôno, Y., Sakashita, S., and Yamazaki, H. (1960*b*).—*Prog. theor. Phys., Kyoto* **24**, 155.

Rogers, M. H. (1956).—*Proc. R. Soc.* A. **235**, 120.

Roxburgh, I. W. (1966).—*Mon. Not. R. astr. Soc.* **132**, 347.

Sakashita, S., and Tanaka, Y. (1962).—*Prog. theor. Phys., Kyoto* **27**, 127.

Whitham, G. B. (1958).—*J. Fluid Mech.* **4**, 337.